

# Scaling Properties of Liquid Dynamics Predicted from a Single Configuration: Pseudoisomorphs for Harmonic-Bonded Molecules

Zahraa Sheydaafar, Jeppe C. Dyre, and Thomas B. Schrøder\*  
*Glass and Time, IMFUFA, Department of Science and Environment,  
Roskilde University, P.O. Box 260, DK-4000 Roskilde, Denmark*  
(Dated: June 18, 2024)

Isomorphs are curves in the thermodynamic phase diagram of invariant excess entropy, structure, and dynamics, while pseudoisomorphs are curves of invariant structure and dynamics, but not of the excess entropy. The latter curves have been shown to exist in molecular models with flexible bonds [Olsen *et al.*, *J. Chem. Phys.* **145**, 241103 (2016)]. We here present three force-based methods to trace out pseudoisomorphs based on a single configuration and test them on the asymmetric dumbbell and 10-bead Lennard-Jones chain models with bonds modeled as harmonic springs. The three methods are based on requiring that particle forces, center-of-mass forces, and torques, respectively, are invariant in reduced units. For each of the two investigated models we identify a method that works well for tracing out pseudoisomorphs.

arXiv:2406.10859v1 [cond-mat.soft] 16 Jun 2024

---

\* tbs@ruc.dk

## I. INTRODUCTION

Defining the excess entropy  $S_{\text{ex}}$  as the entropy minus that of an ideal gas at same density and temperature, isomorphs are curves in the thermodynamic phase diagram along which structure, dynamics, and  $S_{\text{ex}}$  are invariant to a good approximation [1]. Systems with isomorphs, termed R-simple [2–8], are characterized by a strong correlation between the canonical-ensemble equilibrium fluctuations of potential energy  $U$  and virial  $W$  as quantified by the Pearson correlation coefficient (sharp brackets denote canonical averages and  $\Delta$  the deviation from the mean),

$$R = \frac{\langle \Delta W \Delta U \rangle}{\sqrt{\langle (\Delta W)^2 \rangle \langle (\Delta U)^2 \rangle}}. \quad (1)$$

The criterion for being R-simple is  $R > 0.9$  [1], but even systems with somewhat lower  $R$  values may have good isomorphs [9].

Isomorph invariance of structure and dynamics refers to the use of units where the energy unit is  $e_0 \equiv k_B T$ , the length unit is  $l_0 \equiv \rho^{-1/3}$  in which  $\rho$  is the particle number density, and the time unit is  $t_0 \equiv \rho^{-1/3} \sqrt{m/k_B T}$  in which  $m$  is a particle mass. Quantities made dimensionless by reference to this unit system are termed “reduced” and marked by a tilde; for instance the reduced particle position  $\mathbf{r}$  is given by  $\tilde{\mathbf{r}} \equiv \mathbf{r}/l_0 = \rho^{1/3} \mathbf{r}$ .

Because  $S_{\text{ex}}$  is the part of entropy that refers to particle positions, isomorphs are configurational adiabats. These can be traced out in the thermodynamic phase diagram by using the generally valid statistical-mechanical relation [1]:

$$\gamma \equiv \left( \frac{\partial \ln T}{\partial \ln \rho} \right)_{S_{\text{ex}}} = \frac{\langle \Delta U \Delta W \rangle}{\langle (\Delta U)^2 \rangle}. \quad (2)$$

Evaluating the right-hand side by equilibrium  $NVT$  simulations, an isomorph is traced out by solving the differential equation Eq. (2) numerically using, e.g., the Euler or Runge-Kutta methods [10].

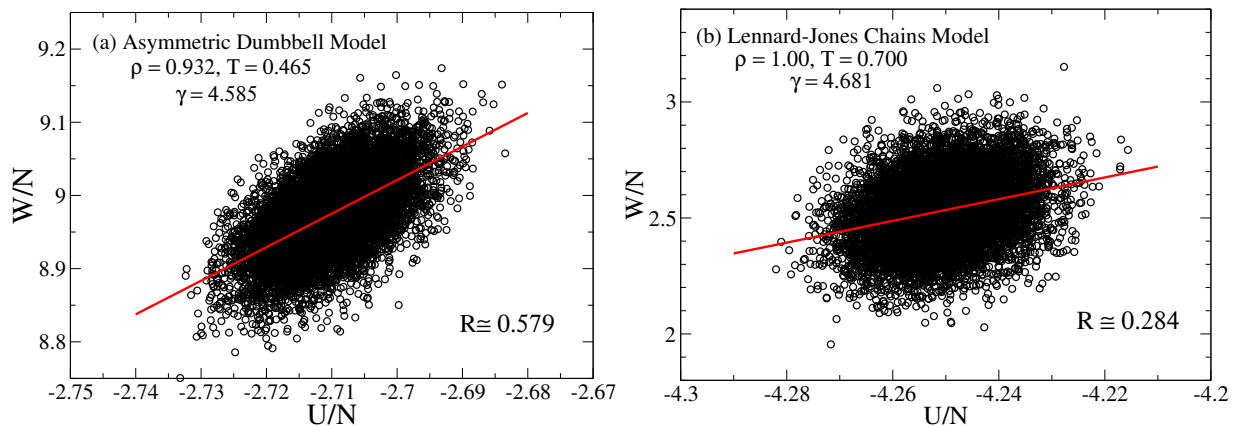


FIG. 1. Scatter plots of equilibrium fluctuations of the virial and the potential energy. (a) Results for the asymmetric dumbbell model with harmonic bonds and (b) for the 10-bead flexible Lennard-Jones chain model with harmonic bonds. For both models the correlation coefficient  $R$  is much smaller than the criterion for an R-simple system,  $R > 0.9$  [1].

Isomorphs have been identified and validated for both atomic [1, 10–14] and molecular systems [9, 15], and isomorph-theory predictions have also been verified in experiments on glass-forming van der Waals molecular liquids [16, 17]. In molecular systems, isomorphs are found when bonds are modeled as constraints [9, 15], but not when the bonds are flexible [8, 18, 19]. As an example, Fig. 1 shows scatter plots of virial versus potential energy for the asymmetric dumbbell (ASD) and 10-bead Lennard-Jones chain (LJC) models, both with harmonic springs as commonly used in simulations [8, 20]. Neither model is R-simple; the virial potential-energy correlation coefficients are 0.579 and 0.284, respectively. As expected, these models do not have isomorphs (data not shown), i.e., structure and dynamics are not invariant along the curves of constant  $S_{\text{ex}}$ . Nevertheless, it has been found that both models have curves in the phase diagram of invariant structure and dynamics; termed “pseudoisomorphs” [8, 15].

Since pseudoisomorphs are not configurational adiabats, Eq. (2) cannot be used to identify such curves in the phase diagram. In 2016 Olsen *et al.* presented a method for tracing out pseudoisomorphs involving the following steps [19]:

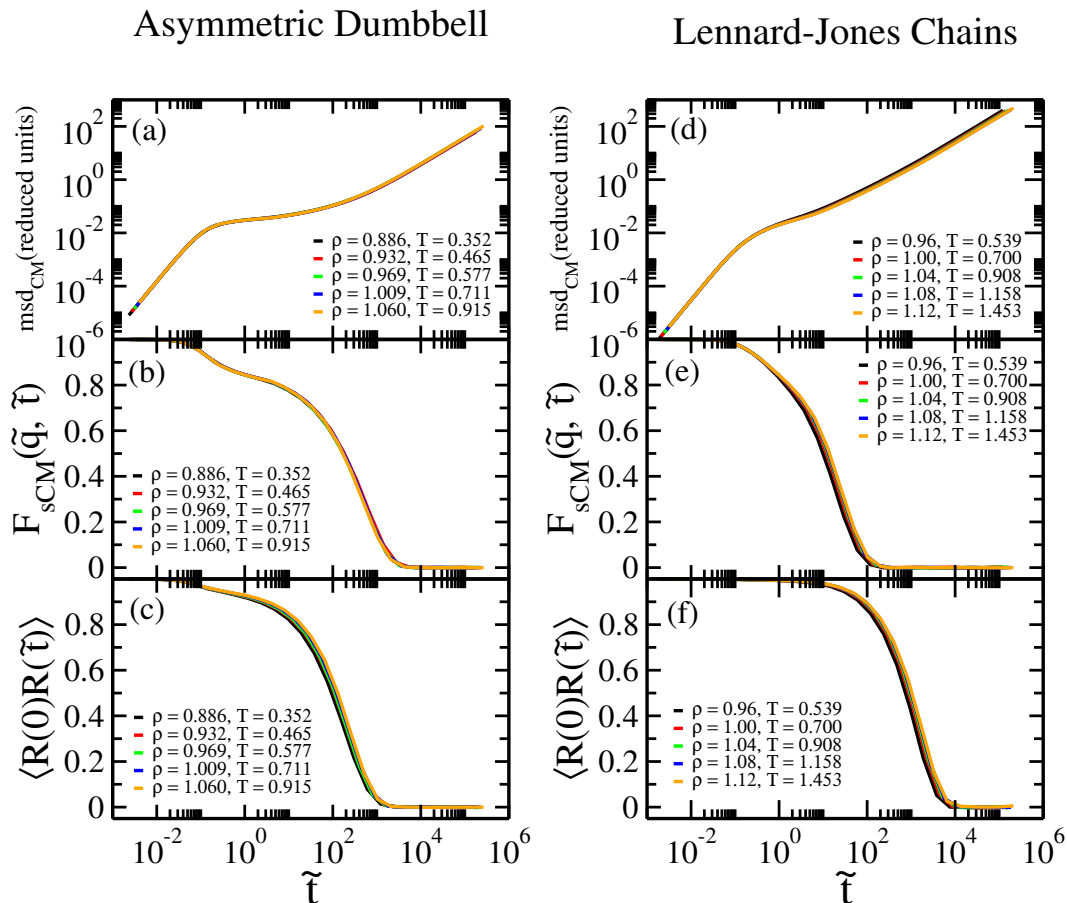


FIG. 2. Invariance of the dynamics along state points determined by Olsen *et al.* [19] to define pseudoisomorphs. (a), (b), (c) show results for the asymmetric dumbbell model with harmonic bonds; (d), (e), (f) show results for the 10-bead Lennard-Jones chain model with harmonic bonds. (a) and (d) report the reduced mean-square displacement of the center of mass as a function of reduced time. (b) and (e) report the center-of-mass incoherent intermediate scattering function as a function of reduced time at the wave-vector corresponding to the first peak of the static structure factor. (c) and (f) report the normalized end-to-end vector time-autocorrelation function, probing the decay of molecular orientation.

1) An equilibrium configuration is quenched to the nearest local minimum in the high-dimensional potential energy landscape, the so-called inherent state [21]; 2) the Hessian matrix is diagonalized to find the vibrational spectrum of the inherent state; 3) the high-frequency part of the spectrum (related to the springs) is identified; 4) the scaling properties upon a density change of the remaining part of the spectrum is used to identify the pseudoisomorph. This method is very computationally demanding, but works well. Olsen *et al.* demonstrated that it traces out pseudoisomorphs for the ASD and the flexible LJC models demonstrating good, though not perfect invariance of the dynamics probed via the incoherent intermediate scattering function. For comparison with later results, Fig. 2 shows the dynamics probed via the mean-square displacement, incoherent intermediate scattering function, and orientational time-autocorrelation function, for the state points identified in [19].

The present paper proposes simpler methods for generating pseudoisomorphs based on the scaling properties of the forces of a single configuration [22]. This idea has been shown to work well not only for atomic systems like the Kob-Andersen binary Lennard-Jones mixture, but also for molecular models like the ASD model and the Lewis-Wahnstrom OTP model with rigid bonds [9, 22–24].

## II. MODELS AND SIMULATION DETAILS

The ASD model is a toy model of toluene [9, 25–32]. We simulated a system of 5000 ASD molecules defined as two different-sized spheres, a large (A) and a small (B) one [25, 33, 34]. The spheres interact via Lennard-Jones (LJ) potentials, and in the units defined by the large sphere ( $\sigma_{AA} \equiv 1$ ,  $\epsilon_{AA} \equiv 1$ , and  $m_A \equiv 1$ ) the other LJ-parameters are

$\sigma_{AB} = 0.894$ ,  $\sigma_{BB} = 0.788$ ,  $\epsilon_{AB} = 0.342$ ,  $\epsilon_{BB} = 0.117$ ,  $m_B = 0.195$ . Bonds are modeled as harmonic springs with equilibrium length 0.584 and spring constant  $k = 3000$ .

The LJC model is a generic coarse-grained polymer model [35–38]. We simulated 1000 10-bead LJC molecules. Non-bonded particles interact via a standard LJ potential, cutting and shifting the forces at  $2.5\sigma$ . All particles are of same type and the potential parameters are set to unity:  $\sigma = 1$ ,  $\epsilon = 1$ . Bonds are modeled as harmonic springs with equilibrium length 1 and spring constant  $k = 3000$ .

All Molecular Dynamics simulations were performed in the *NVT* ensemble with a Nose-Hoover thermostat in periodic boundary conditions, using RUMD that is an open-source molecular dynamics package optimized for GPU computing [39] (<http://rumd.org>).

### III. IDENTIFYING PSEUDOISOMORPHS VIA FORCE-BASED METHODS

Single-configuration force-based methods for generating isomorphs were introduced recently [22, 24]. The idea is the following. Given a configuration  $\mathbf{R}_1$  at state point  $(\rho_1, T_1)$ , a uniform scaling to density  $\rho_2$  is performed leading to  $\mathbf{R}_2 = (\rho_1/\rho_2)^{1/3} \mathbf{R}_1$ . For molecules, two variants of this scaling can be applied: “center-of-mass scaling” where the molecular center-of-masses are scaled while all orientations and internal degrees of freedom are kept fixed, or “atomic scaling” where a uniform scaling is applied to all atoms thus modifying also the intramolecular bond lengths. After scaling a configuration, the forces associated with the two configurations,  $\mathbf{F}(\mathbf{R}_1)$  and  $\mathbf{F}(\mathbf{R}_2)$ , are compared ( $\mathbf{F}$  is the long vector of all forces). The temperature  $T_2$  at the density  $\rho_2$  is identified from the condition of invariant reduced forces. Specifically,  $|\tilde{\mathbf{F}}(\mathbf{R}_1)| = |\tilde{\mathbf{F}}(\mathbf{R}_2)|$  implies [22]

$$T_2 = \frac{|\mathbf{F}(\mathbf{R}_2)|}{|\mathbf{F}(\mathbf{R}_1)|} \left( \frac{\rho_1}{\rho_2} \right)^{1/3} T_1. \quad (3)$$

If the two force vectors are parallel, this leads to the forces being identical in reduced units,  $\tilde{\mathbf{F}}(\mathbf{R}_1) = \tilde{\mathbf{F}}(\mathbf{R}_2)$ . Assuming this is representative of all relevant configurations, it follows that structure and dynamics are invariant in reduced units because the same reduced-unit equation of motion applies at the two state points [5, 40]. We do not expect the force vectors before and scaling to be perfectly parallel, however, but Eq. (3) can still be used. Reference [22] proposed that for force-based method to work well, the standard Pearson as well as Spearman (ordering) correlation coefficients of the force components should both be larger than 0.95.

Different variants of the method are arrived at by different interpretations of what exactly  $\mathbf{F}(\mathbf{R})$  represents, e.g., the forces on all the atoms or just on the center-of-mass forces. We consider below also a variant based on invariance of torques in reduced units,  $\tilde{\boldsymbol{\tau}}_1 = \tilde{\boldsymbol{\tau}}_2$ , which leads to

$$T_2 = \frac{|\boldsymbol{\tau}_2|}{|\boldsymbol{\tau}_1|} T_1. \quad (4)$$

The three methods are applied to the ASD model in Fig. 3, using center-of-mass scaling, i.e.,  $\mathbf{R}_{2,cm} = (\rho_1/\rho_2)^{1/3} \mathbf{R}_{1,cm}$ . The state point  $(\rho_1, T_1) = (0.785, 0.174)$  is used as reference and  $\rho_2 = 0.856$ , i.e., a 9% density increase is considered. Figure 3(a) shows a scatter plot of the atomic-force components before and after scaling for a single configuration; here  $T_2 = 0.197$  is found by applying atomic forces in Eq. (3). Figure 3(b) shows a similar plot based on the center-of-mass “molecular” forces. In this case the quite different  $T_2 = 0.299$  is arrived at and a significantly better correlation is obtained. Finally, Fig. 3(c) shows the torque correlations of molecules of unscaled and scaled configurations. The correlation is here not far from that of the molecular forces; using Eq. (4) gives  $T_2 = 0.310$ .

For each of the three methods, Fig. 4 compares results for the dynamics. While the methods in principle require only a single configuration, for carefully comparing the methods,  $T_2$ -values were obtained by averaging over 195 independent configurations. We find that the molecular-force method gives almost invariant dynamics, except at the lowest density (black curve) where negative pressure and phase separation is observed. The torque method gives similar, though slightly inferior results, while the atomic force method does not work well.

Next we turn to the 10-bead harmonic-spring LJC model for which one can use not only the three above methods, but also a fourth one based on invariant reduced segmental forces. These are defined as

$$\mathbf{F}_{Seg,j} \equiv \frac{1}{d_j} \mathbf{F}_j + \frac{1}{d_{j+1}} \mathbf{F}_{j+1}, \quad (5)$$

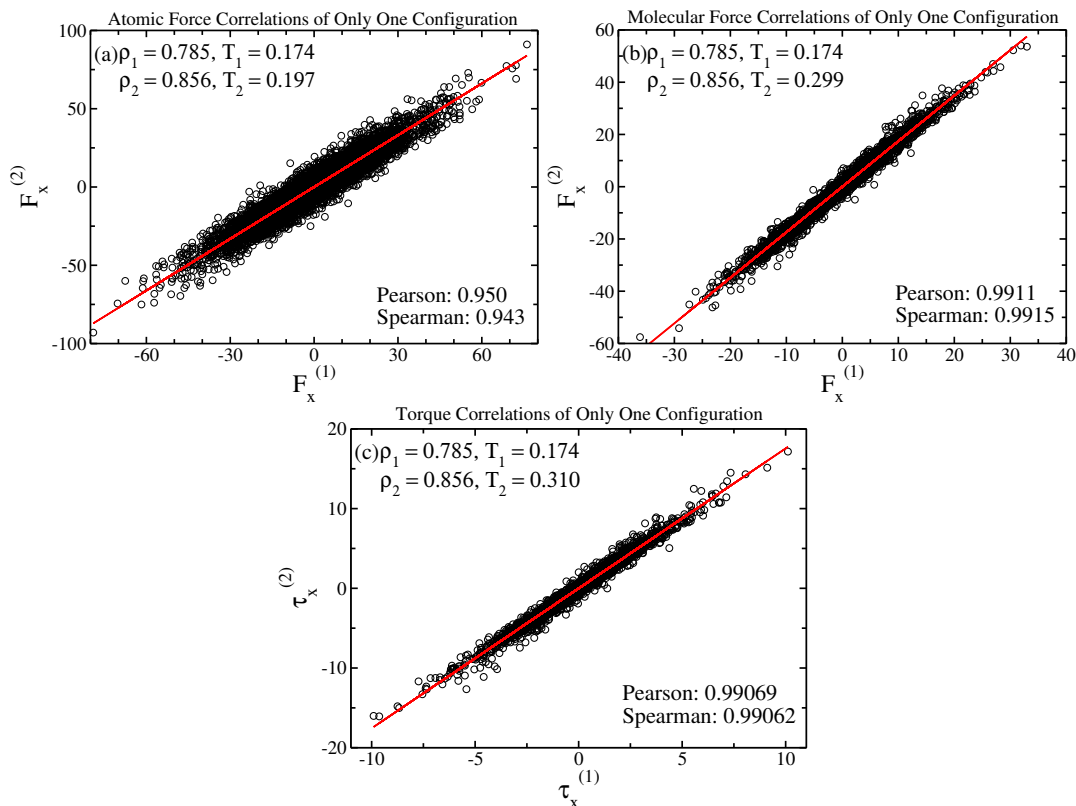


FIG. 3. Force and torque correlations of a single configuration of the harmonic ASD model using center-of-mass scaling. Each point represents scaled and unscaled forces/torques. (a) Atomic-force method. The figure shows the x-coordinates of the reduced particle forces plotted against the same quantities of the uniformly scaled configuration. The temperature  $T_2 = 0.197$  is identified by means of Eq. (3). (b) Molecular-force method. The figure shows the center-of-mass “molecular” forces before and after scaling, which have no contributions from the springs. In this case  $T_2 = 0.299$ . (c) Torque method. The figure shows the correlation between the torques of the molecules before and after scaling ( $T_2 = 0.310$ ).

in which  $d_j$  and  $d_{j+1}$  are the number of bonds that particles  $j$  and  $j + 1$  are involved in. Clearly

$$\mathbf{F}_{Mol} = \sum_{j=1}^9 \mathbf{F}_{Seg,j}. \quad (6)$$

The results are quite different from the ASD results. Thus the dynamics are to a good approximation invariant for the atomic- and segmental-force methods (Fig. 5 (g), (h), (i)), except at the lowest density from reference point  $(\rho_1, T_1) = (1.00, 0.700)$  at which the virial becomes negative. On the other hand, neither the molecular force method (d, e, f) nor the torque method (j, k, l) produce good pseudoisomorphs.

#### IV. PSEUDOISOMORPHS IN THE ASD MODEL AT HIGHER DENSITIES

In Fig. 4 we applied the three force-based single-configuration methods to the ASD model and found best invariance of the dynamics using the molecular-force and, to a slightly less degree, torque methods. Figure 6 shows the results of applying the three methods at higher densities. The invariance of the dynamics is not as good as at lower densities (Fig. 4). The molecular-force method works best, but no method works as well as the method of Ref. 19, compare Fig. 2.

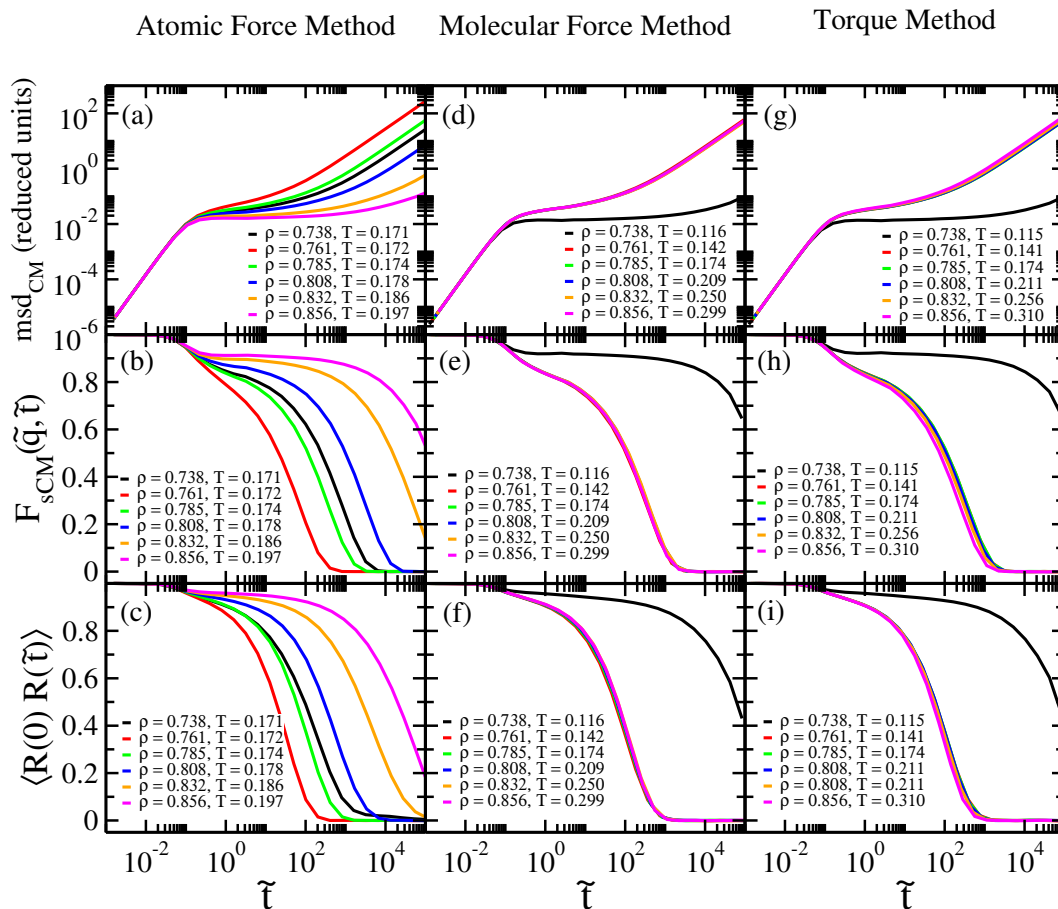


FIG. 4. Testing for invariance of the reduced dynamics of the harmonic-spring ASD model using the three methods generating pseudoisomorphs by scaling a single configuration of the reference state point  $(\rho_1, T_1) = (0.785, 0.174)$ . Each method investigates the reduced center-of-mass mean-square displacement (upper figures), center-of-mass incoherent intermediate scattering function at the wave vectors corresponding to the first peak of the static structure factor (middle figures), and directional time-autocorrelation function probed via the autocorrelation function of the normalized bond vectors (bottom figures). (a), (b), (c) show results of the atomic-force method requiring invariant reduced forces between all atoms, i.e., including the harmonic bond contributions into Eq. (3). (d), (e), (f) show results of the molecular-force method requiring invariant reduced center-of-mass forces between the molecules. (g), (h), (i) show results of the torque method requiring invariant reduced torques on the molecules (Eq. (4)).

### A. What is the problem?

Figure 7(a) shows the distributions of bond lengths for simulations at the state points generated by the molecular-force method. The bonds are compressed when the density is increased, an effect that is not seen at the lower densities of Fig. 4. This means that when a configuration from the reference state point is scaled to a higher density, the scaled configuration is not representative of equilibrium configurations at the new state point because the bonds are too long, an issue that becomes more serious at higher densities.

To eliminate the effects of the harmonic bonds, we introduce the following procedure: For a given configuration fix the center-of-mass and orientation of each molecule. For this “constrained” system add a length  $l$  to all bond lengths and minimize the potential energy with respect to  $l$ . We refer to this procedure as “quenching”, but note that the minimization only involves a single variable, the length  $l$  added to all bonds. When applied to an unscaled configuration, the bond length distribution remains largely unchanged (black and orange curves in Fig. 7 (b)). Now, consider the scaling of the original configuration to higher density, with the aim to achieve a bond length distribution close to that of the equilibrium at the new state point (green curve). Using center-of-mass scaling of the molecules leaves the bond lengths unchanged (black curve), whereas atomic scaling lead to too small bond lengths (red curve). Applying the quenching procedure after center-of-mass scaling shifts the distribution to shorter bond lengths (from the black line to the blue line), and the average bond length approaches that of the equilibrium distribution at the

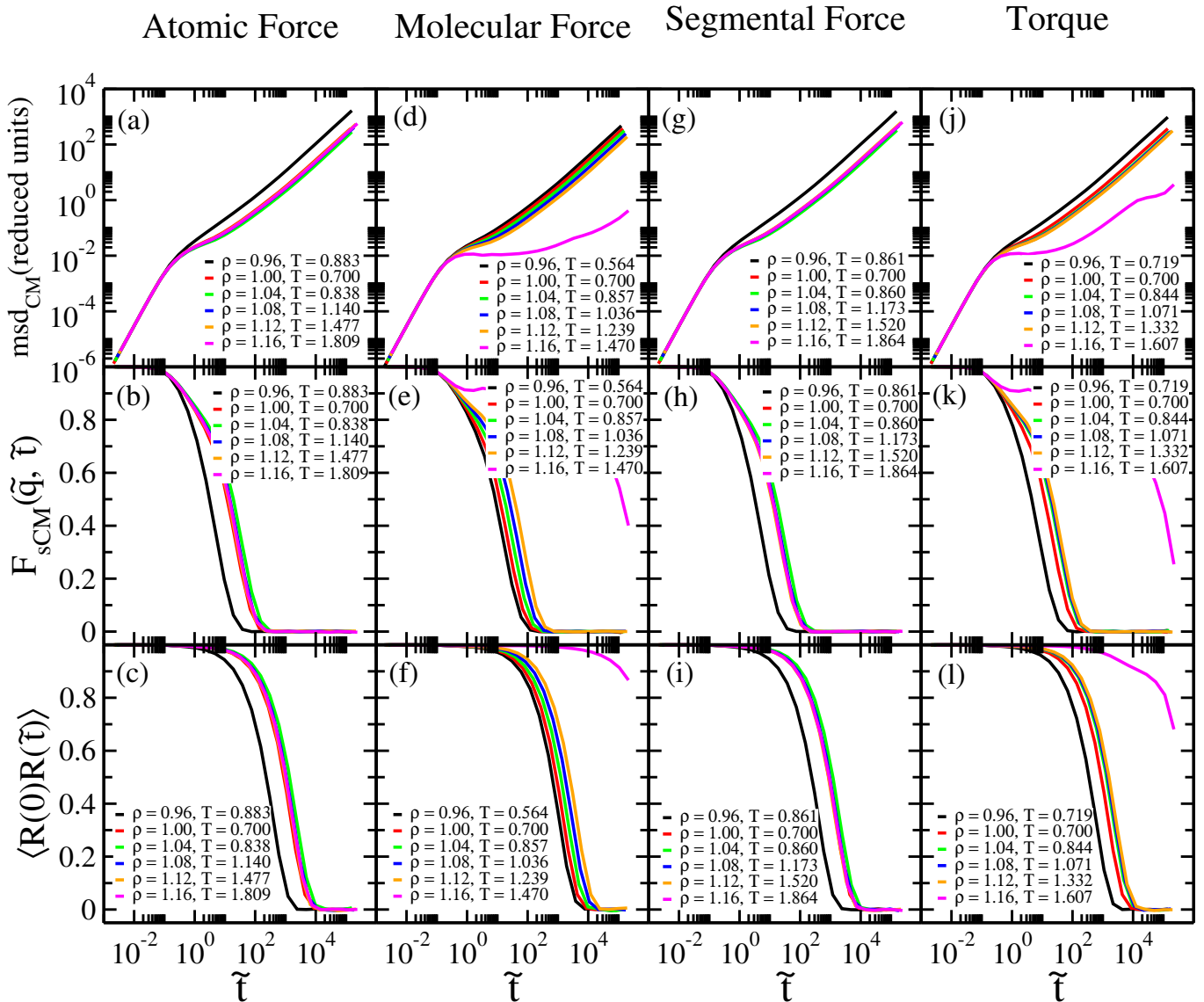


FIG. 5. Dynamics of the harmonic-spring LJC model along proposed pseudoisomorphs. The reference state point is  $(\rho_1, T_1) = (1.00, 0.700)$  and the density increase is 17%. The atomic-force and molecular-force methods both generate good pseudoisomorphs when increasing density as compared to the reference state point. For both methods, decreasing the density leads to a higher temperature, which obviously leads to too fast dynamics. The torque method results in better invariance than the molecular-force method for a range of densities, but worse than the atomic-force and segmental-force methods.

higher density (green line). This effectively eliminates the non-scaling degrees of freedom thought to cause the poor invariance observed in Fig. 6.

Based on pairs of quenched configurations, one may again apply the atomic-force, molecular-force, and torque methods to generate state points with, hopefully, same dynamics. Specifically, we proceeded as follows. A single configuration is selected from an equilibrium simulation at the reference state point (density  $\rho_1$ ). This configuration is scaled uniformly to the density of interest,  $\rho_2$ . Both scaled and unscaled configurations were then quenched as described above in order to eliminate the bond vibrational degrees of freedom. After this the relevant forces / torques were evaluated and  $T_2$  determined from Eq. (3) and Eq. (4), respectively. Figure 8(a) shows the forces of a single scaled configuration versus those of the unscaled configuration before quenching, while (b) demonstrates better correlation after quenching; (c) and (d) show the correlations between the center-of-mass forces before and after quenching. The quench method leads to significantly better correlation, with correlation coefficient increasing from 0.850 to 0.934 in the atomic-force case and from 0.975 to 0.990 in the molecular (center-of-mass) force case.



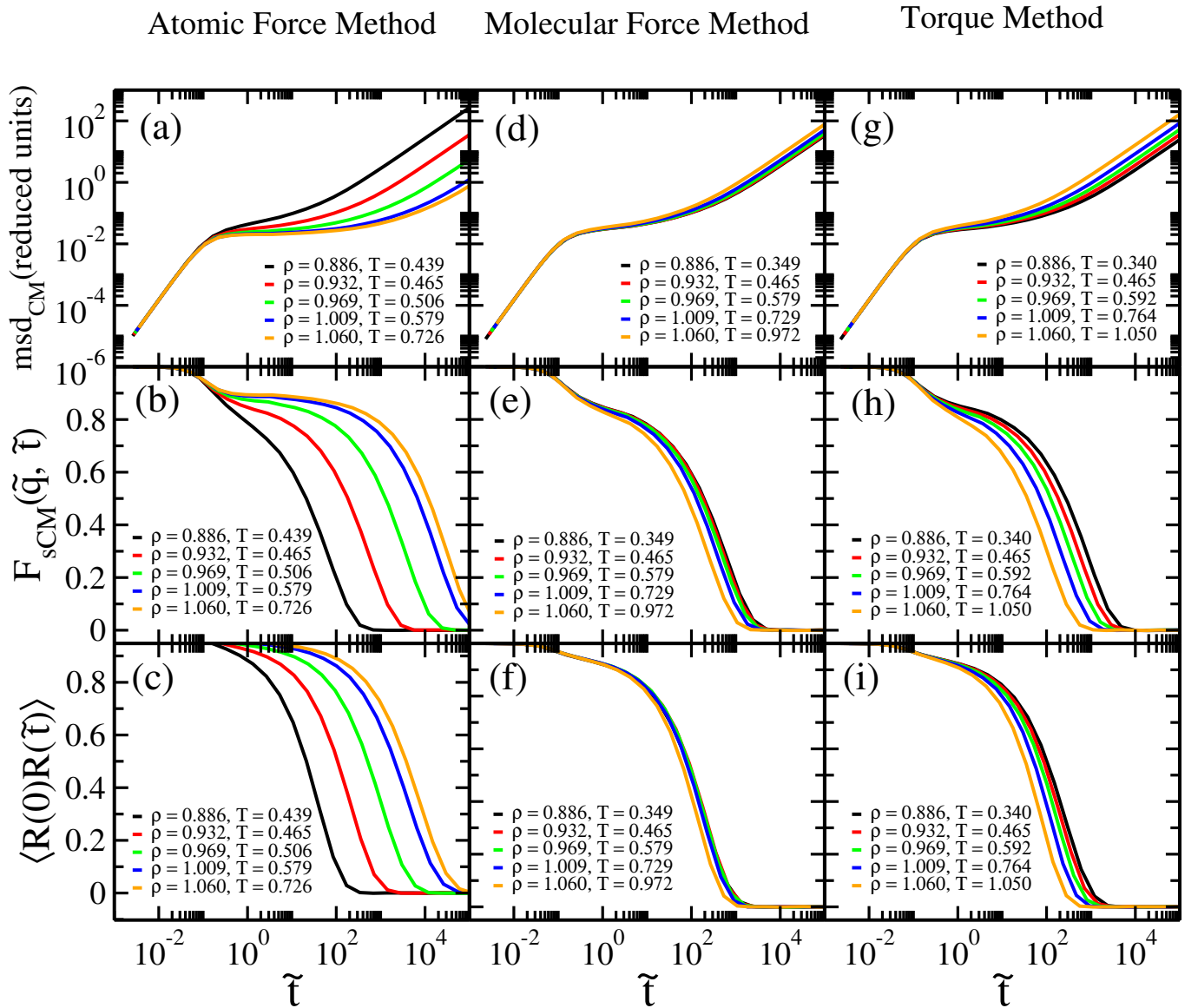


FIG. 6. Dynamics of the ASD model along proposed pseudoisomorphs. The densities are here higher than in Fig. 4. The density increase is 19%. For all three methods center-of-mass scaling was employed. The reference state point  $(\rho_1, T_1) = (0.932, 0.465)$  is taken from Ref. [19]. The molecular-force methods works best, but the invariance is not as good as at lower densities (Fig. 4).

The effect of the quenching procedure is tested in Fig. 9, which is analogous to Fig. 6 except that the temperatures  $T_2$  are calculated based on quenched configurations. The best results are obtained with the molecular-force method, which was also the one that worked best in Fig. 4. For this method we find excellent collapse of the reduced center-of-mass mean-square displacement as a function of time, as well as of the center-of-mass incoherent intermediate scattering function. The directional time-autocorrelation function shows a slightly worse collapse, but is nevertheless significantly better than without quenching. Comparing the results of the torque method with and without quenching shows that quenching also here significantly improves the invariances. – Using atomic scaling gives the same results for the molecular force and torque methods after the system has been quenched (Table I), while the atomic-force method gives results different from Fig. 9.



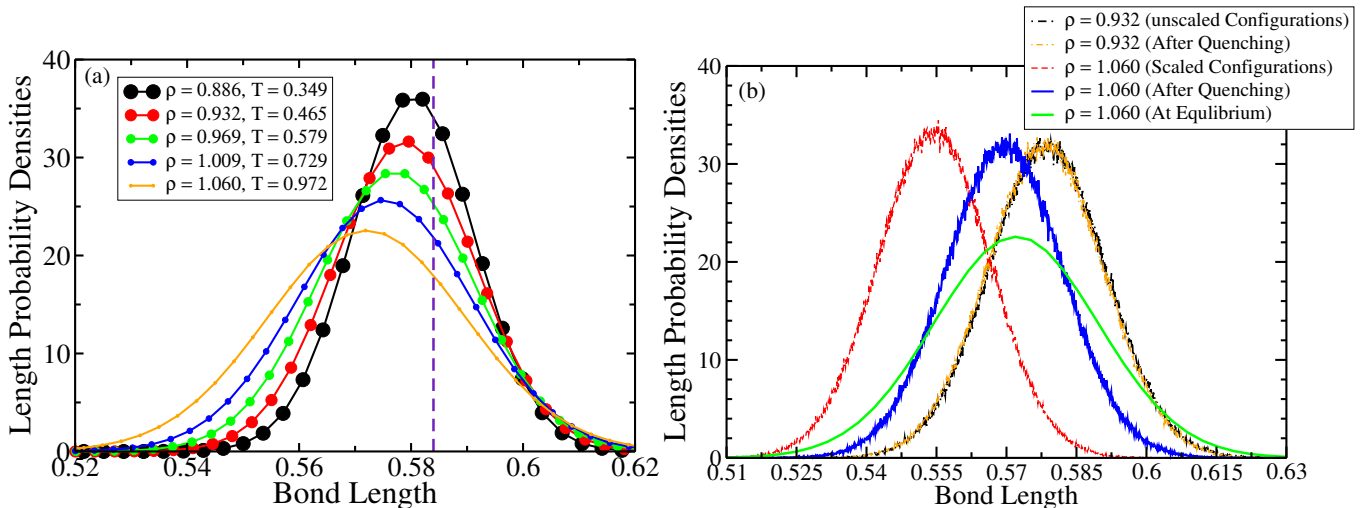


FIG. 7. (a) Equilibrium distribution of ASD bond lengths at state points identified by the molecular-force method (see Figure 6(d,e,f)). Bonds are compressed when density is increased. This means that when a configuration is center-of-mass scaled from the reference state point to a (say) higher density, the resulting configuration is not representative of the equilibrium configurations at this higher density. (b) Quenching the system according to the constraint conditions (fixed centre-of-mass and orientational direction of all molecules). Black: bond length distribution of original unscaled configuration at the reference state point. Orange: applying the quenching procedure to the unscaled configuration leads to virtually the same distribution. Red: atomic scaling to the new higher density leads to bond lengths that are considerably smaller than the ones in equilibrium at the new state point (green curve). Blue: center-of-mass scaling to the new higher density followed by the quenching procedure leads to a bond length distribution that is close to the one in equilibrium at the new state point (green curve). Note: the procedure adds the same length 'l' to all bonds, which lead to shift in the distribution leaving the shape invariant.

TABLE I. Predicted temperature using atomic scaling after quenching (ASD model). Note that the molecular-force and torque methods give the same results as when center-of-mass scaling is used (Fig. 9).  $\rho = 0.932$  is the reference density in all cases.

density	$T(F_{Atomic})$	$T(F_{Mol})$	Torque
0.886	0.444	0.352	0.345
0.932	0.465	0.465	0.465
0.969	0.494	0.573	0.581
1.009	0.540	0.710	0.730
1.060	0.624	0.917	0.957

## V. SUMMARY

Genuine isomorphs do not exist in systems without strong virial potential-energy correlations, e.g., systems of molecules with harmonic bonds. For the ASD model and the flexible LJC model with harmonic bonds curves nevertheless exist along which the structure and dynamics are invariant to a good approximation, so-called pseudoisomorphs [19]. These curves do not have invariant excess entropy, but otherwise behave much like isomorphs by having approximately invariant structure and dynamics in reduced units. A previously discussed method for tracing out pseudoisomorphs in the thermodynamic phase diagram works well, but is quite complicated to apply in practice [19]. The present paper explored the possibility of tracing out pseudoisomorphs based on the simple requirement of invariant length of the reduced force vector of a single configuration after scaling. Although the focus above was on the dynamics, we note that for all three methods discussed the structure is also invariant to a good approximation, both with and without quenching (Fig. 10).

For the harmonic-bond ASD model the best method for tracing out pseudoisomorphs is the molecular-force method with center-of-mass scaling and quenching of the harmonic bonds (Fig. 9). At low densities, the quenching can be skipped (Fig. 4). We conjecture that this method will work on all small molecules with harmonic bonds, assuming of course that the systems in question have pseudoisomorphs. The molecular-force method does not work well for the 10-bead harmonic-bond LJ-chain model, however, for which the best method is the atomic-force method with atomic scaling (Fig. 5).

From a practical point of view one would like to have a single method that works for all molecular models with

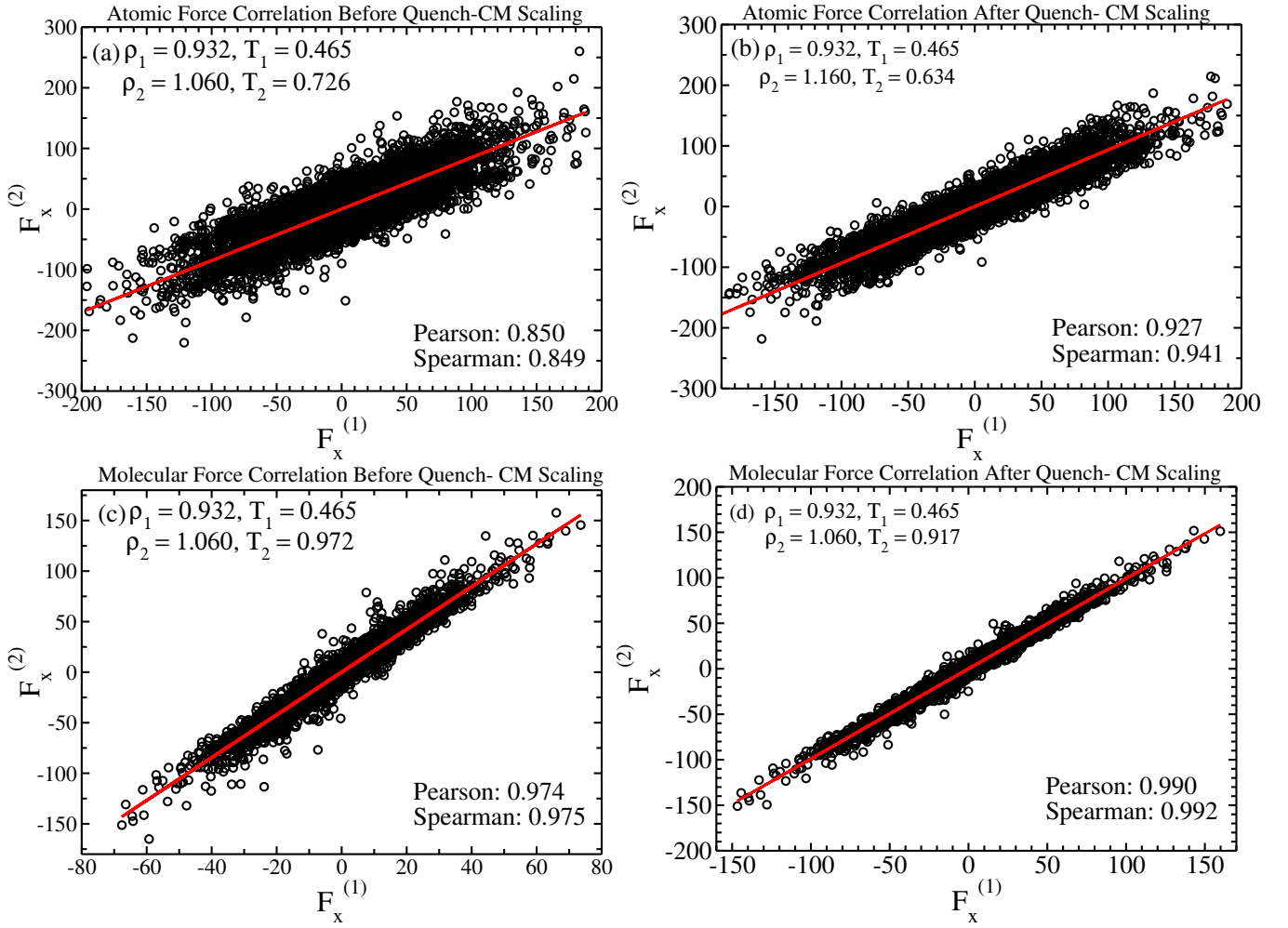


FIG. 8. Correlation of atomic-force components, (a) and (b), and molecular-force components, (c) and (d), for the ASD model. A configuration is taken from a simulation at  $(\rho_1, T_1) = (0.932, 0.465)$  and  $T_2$  as previously calculated by means of Eq. (3). For both the atomic-force and molecular-force methods we find significantly better correlations between scaled and non-scaled forces components when applying a quench. Note that only the molecular forces fulfill the criterion that the Pearson and Spearman correlation coefficients are both above 0.95 [22].

pseudoisomorphs, including the two models investigated here. The differences found can be interpreted as reflecting differences regarding which forces are important for the motion of the molecules. Despite the harmonic bonds, the ASD is relatively stiff and its motion is largely governed by the center-of-mass “molecular” force and the torque. If the scaling were perfect, both the molecular-force and the torque methods would lead to invariant dynamics. The fact that we find the molecular-force method to work better than the torque method can be interpreted as the molecular forces being more important than the torques for the motion of the molecules. It would be interesting to investigate whether molecular models exist for which the torque method works better than the molecular-force method. The molecular-force method does not work well for the LJC model. We interpret this as reflecting the fact that the center-of-mass motion does not determine the motion of this complex, flexible molecule, which should rather be thought of in terms of the motion of its beads.

In summary, simple single-configuration force-based methods exist for tracing out pseudoisomorphs, which work as well as the complicated method of diagonalizing the Hessian before and after scaling.[19] No single-configuration method of general validity has been identified, however. More work is needed to investigate these and other methods. In this regard, we find it encouraging that the introduction of quenches after scaling improves all the methods studied.

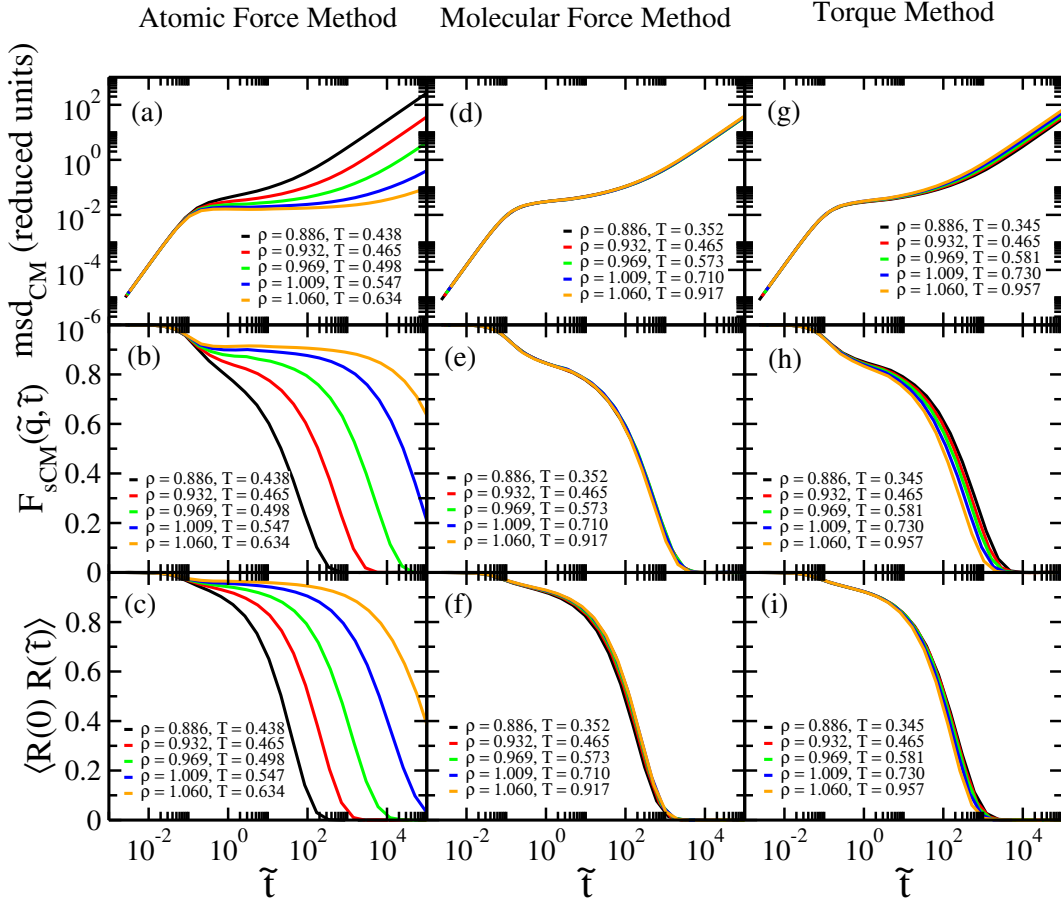


FIG. 9. Testing the ASD model for invariance of the reduced dynamics using the three quench methods for generating pseudoisomorphs based on a single configuration from  $(\rho_1, T_1) = (0.932, 0.465)$ . In contrast to Fig. 6, the scaled and non-scaled configurations were here quenched to a potential-energy minimum in order to eliminate the harmonic bond degrees of freedom; after which  $T_2$  was determined as in Fig. 6.

#### ACKNOWLEDGMENTS

This work was supported by the VILLUM Foundation's *Matter* grant (VIL16515).

- 
- [1] N. Gnan, T. B. Schröder, U. R. Pedersen, N. P. Bailey, and J. C. Dyre, Pressure-energy correlations in liquids. IV. “Isomorphs” in liquid phase diagrams, *J. Chem. Phys.* **131**, 234504 (2009).
  - [2] A. Malins, J. Eggers, and C. P. Royall, Investigating isomorphs with the topological cluster classification, *J. Chem. Phys.* **139**, 234505 (2013).
  - [3] E. Flenner, H. Staley, and G. Szamel, Universal Features of Dynamic Heterogeneity in Supercooled Liquids, *Phys. Rev. Lett.* **112**, 097801 (2014).
  - [4] S. Prasad and C. Chakravarty, Onset of simple liquid behaviour in modified water models, *J. Chem. Phys.* **140**, 164501 (2014).
  - [5] T. B. Schröder and J. C. Dyre, Simplicity of condensed matter at its core: Generic definition of a Roskilde-simple system, *J. Chem. Phys.* **141**, 204502 (2014).
  - [6] D. M. Heyes, D. Dini, and A. C. Branka, Scaling of Lennard-Jones liquid elastic moduli, viscoelasticity and other properties along fluid-solid coexistence, *Phys. Status Solidi (b)* **252**, 1514 (2015).
  - [7] S. A. Khrapak, B. Klumov, L. Couedel, and H. M. Thomas, On the long-waves dispersion in Yukawa systems, *Phys. Plasmas* **23**, 023702 (2016).
  - [8] F. Kaskosz, K. Koperwas, A. Grzybowski, and M. Paluch, The origin of the density scaling exponent for polyatomic molecules and the estimation of its value from the liquid structure, *J. Chem. Phys.* **158**, 144503 (2023).

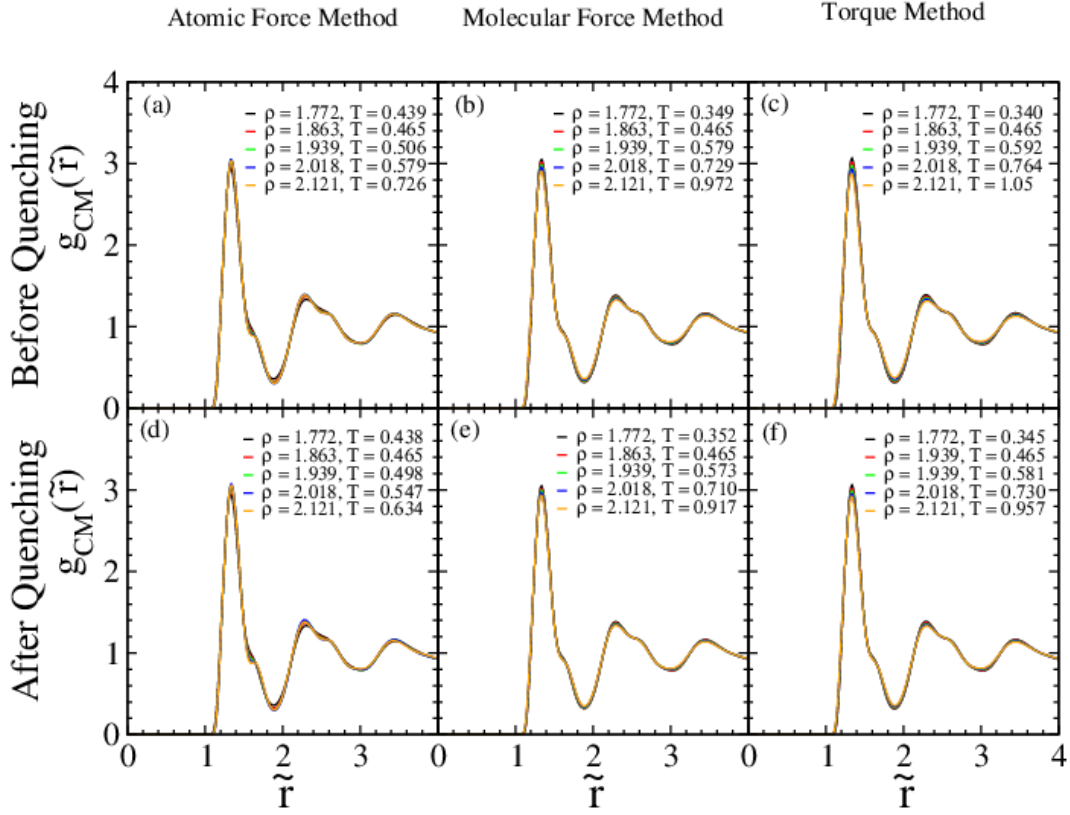


FIG. 10. Testing the ASD model for invariance of the reduced-unit radial distribution function for the three different methods, without and with quenching, using  $(\rho_1, T_1) = (0.932, 0.465)$  as reference state point. (a), (b), (c) show results for state points generated by the atomic-force, molecular-force, and torque methods; (d), (e), (f) show results for state points generated by the same methods after minimization. In all cases, structure is invariant to a good approximation.

- [9] T. S. Ingebrigtsen, T. B. Schröder, and J. C. Dyre, Isomorphs in model molecular liquids, *J. Phys. Chem. B* **116**, 1018 (2012).
- [10] E. Attia, J. C. Dyre, and U. R. Pedersen, Extreme case of density scaling: The Weeks-Chandler-Andersen system at low temperatures, *Phys. Rev. E* **103**, 062140 (2021).
- [11] L. Böhling, T. S. Ingebrigtsen, A. Grzybowski, M. Paluch, J. C. Dyre, and T. B. Schröder, Scaling of viscous dynamics in simple liquids: Theory, simulation and experiment, *New J. Phys.* **14**, 113035 (2012).
- [12] A. K. Bacher, T. B. Schröder, and J. C. Dyre, The EXP pair-potential system. II. Fluid phase isomorphs, *J. Chem. Phys.* **149**, 114502 (2018).
- [13] D. M. Heyes, D. Dini, L. Costigliola, and J. C. Dyre, Transport coefficients of the Lennard-Jones fluid close to the freezing line, *J. Chem. Phys.* **151**, 204502 (2019).
- [14] F. L. Castello, P. Tolias, and J. C. Dyre, Testing the isomorph invariance of the bridge functions of Yukawa one-component plasmas, *J. Chem. Phys.* **154**, 034501 (2021).
- [15] A. A. Veldhorst, J. C. Dyre, and T. B. Schröder, Scaling of the dynamics of flexible Lennard-Jones chains, *J. Chem. Phys.* **141**, 054904 (2014).
- [16] W. Xiao, J. Tofteskov, T. V. Christensen, J. C. Dyre, and K. Niss, Isomorph theory prediction for the dielectric loss variation along an isochrone, *J. Non-Cryst. Solids* **407**, 190 (2015).
- [17] H. W. Hansen, A. Sanz, K. Adrjanowicz, B. Frick, and K. Niss, Evidence of a one-dimensional thermodynamic phase diagram for simple glass-formers, *Nat. Commun.* **9**, 518 (2018).
- [18] A. A. Veldhorst, J. C. Dyre, and T. B. Schröder, Scaling of the dynamics of flexible Lennard-Jones chains: Effects of harmonic bonds, *J. Chem. Phys.* **143**, 194503 (2015).
- [19] A. E. Olsen, J. C. Dyre, and T. B. Schröder, Communication: Pseudoisomorphs in liquids with intramolecular degrees of freedom, *J. Chem. Phys.* **145**, 241103 (2016).
- [20] K. Koperwas and M. Paluch, Computational evidence for the crucial role of dipole cross-correlations in polar glass-forming liquids, *Phys. Rev. Lett.* **129**, 025501 (2022).
- [21] F. H. Stillinger and T. A. Weber, Dynamics of structural transitions in liquids, *Phys. Rev. A* **28**, 2408 (1983).
- [22] T. B. Schröder, Predicting scaling properties from a single fluid configuration, *Phys. Rev. Lett.* **129**, 245501 (2022).
- [23] K. Koperwas, A. Grzybowski, and M. Paluch, Virial-potential-energy correlation and its relation to density scaling for

- quasireal model systems, *Phys. Rev. E* **102**, 062140 (2020).
- [24] Z. Sheydaafar, J. C. Dyre, and T. B. Schröder, Scaling properties of liquid dynamics predicted from a single configuration: Small rigid molecules, *J. Phys. Chem. B* **127**, 3478 (2023).
- [25] J. Vrabec, J. Stoll, and H. Hasse, A set of molecular models for symmetric quadrupolar flu, *J. Phys. Chem. B* **105**, 12126 (2001).
- [26] A. L. Galbraith and C. K. Hall, Solid–liquid phase equilibria for mixtures containing diatomic Lennard–Jones molecules, *Fluid Phase Eq.* **262**, 1 (2007).
- [27] T. B. Schröder, N. P. Bailey, U. R. Pedersen, N. Gnan, and J. C. Dyre, Pressure-energy correlations in liquids. III. Statistical mechanics and thermodynamics of liquids with hidden scale invariance, *J. Chem. Phys.* **131**, 234503 (2009).
- [28] R. Chopra, T. M. Truskett, and J. R. Errington, Excess-entropy scaling of dynamics for a confined fluid of dumbbell-shaped particles, *Phys. Rev. E* **82**, 041201 (2010).
- [29] R. Chopra, T. M. Truskett, and J. R. Errington, Excess entropy scaling of dynamic quantities for fluids of dumbbell-shaped particles, *J. Chem. Phys.* **133**, 104506 (2010).
- [30] D. Fragiadakis and C. M. Roland, A test for the existence of isomorphs in glass-forming materials, *J. Chem. Phys.* **147**, 084508 (2017).
- [31] I. Santiago, Nanoscale active matter matters: Challenges and opportunities for self-propelled nanomotors, *Nano Today* **19**, 11 (2018).
- [32] T. Dombrowski and D. Klotsa, Kinematics of a simple reciprocal model swimmer at intermediate Reynolds numbers, *Phys. Rev. Fluids* **5**, 063103 (2020).
- [33] T. B. Schröder, U. R. Pedersen, N. P. Bailey, S. Toxvaerd, and J. C. Dyre, Hidden Scale Invariance in Molecular van der Waals Liquids: A Simulation Study, *Phys. Rev. E* **80**, 041502 (2009).
- [34] K. Milinkovic, M. Dennison, and M. Dijkstra, Phase diagram of hard asymmetric dumbbell particles, *Phys. Rev. E* **87**, 032128 (2013).
- [35] C. Bennemann, W. Paul, K. Binder, and B. Dünweg, Molecular-dynamics simulations of the thermal glass transition in polymer melts:  $\alpha$ -relaxation behavior, *Phys. Rev. E* **57**, 843 (1998).
- [36] M. Aichele, Y. Gebremichael, F. W. Starr, J. Baschnagel, and S. C. Glotzer, Polymer-specific effects of bulk relaxation and stringlike correlated motion in the dynamics of a supercooled polymer melt, *J. Chem. Phys.* **119**, 5290 (2003).
- [37] F. Puosi and D. Leporini, Scaling between relaxation, transport, and caged dynamics in polymers: From cage restructuring to diffusion, *J. Phys. Chem. B* **115**, 14046 (2011).
- [38] A. Shavit, J. F. Douglas, and R. A. Riggleman, Evolution of collective motion in a model glass-forming liquid during physical aging, *J. Chem. Phys.* **138**, 12A528 (2013).
- [39] N. P. Bailey, T. S. Ingebrigtsen, J. S. Hansen, A. A. Veldhorst, L. Bøhling, C. A. Lemarchand, A. E. Olsen, A. K. Bacher, L. Costigliola, U. R. Pedersen, H. Larsen, J. C. Dyre, and T. B. Schröder, RUMD: A general purpose molecular dynamics package optimized to utilize GPU hardware down to a few thousand particles, *SciPost Phys.* **3**, 038 (2017).
- [40] J. C. Dyre, Perspective: Excess-entropy scaling, *J. Chem. Phys.* **149**, 210901 (2018).